Published in final edited form as:
Sci Transl Med. 2011 June 29; 3(89): 89ra57. doi:10.1126/scitranslmed.3002156.

Human apoE isoforms differentially regulate brain amyloid-β peptide clearance

Joseph M. Castellano[1,2,3,10], **Jungsu Kim**[1,2,3,10], **Floy R. Stewart**[1,2,3], **Hong Jiang**[1,2,3], **Ronald B. DeMattos**[4], **Bruce W. Patterson**[5], **Anne M. Fagan**[1,2,3], **John C. Morris**[1,3], **Kwasi G. Mawuenyega**[1,2,3], **Carlos Cruchaga**[2,3,6], **Alison M. Goate**[1,2,3,6], **Kelly R. Bales**[7], **Steven M. Paul**[8], **Randall J. Bateman**[1,2,3], and **David M. Holtzman**[1,2,3,9,*]

[1]Department of Neurology, Washington University School of Medicine, St. Louis, MO 63110, USA

[2]Hope Center for Neurological Disorders, Washington University School of Medicine, St. Louis, MO 63110, USA

[3]Charles F. and Joanne Knight Alzheimer's Disease Research Center, Washington University School of Medicine, St. Louis, MO 63110, USA

[4]Eli Lilly & Co., Lilly Research Labs, Indianapolis, IN 46285, USA

[5]Department of Internal Medicine, Washington University School of Medicine, St. Louis, MO 63110, USA

[6]Department of Psychiatry, Washington University School of Medicine, St. Louis, MO 63110, USA

[7]Neuroscience Research Unit, Pfizer Global Research & Development, Groton, CT 06430, USA

[8]Appel Alzheimer's Disease Research Institute, Weill Cornell Medical College, Cornell University, New York, NY 10065, USA

[9]Department of Developmental Biology, Washington University School of Medicine, St. Louis, MO 63110, USA

Abstract

The apolipoprotein E (*APOE*) ε4 allele is the strongest genetic risk factor for late-onset, sporadic Alzheimer's disease (AD). The *APOE* ε4 allele dramatically increases AD risk and decreases age of onset, likely through its strong effect on the accumulation of amyloid-β (Aβ) peptide. In contrast, the *APOE* ε2 allele appears to decrease AD risk. Most rare, early-onset forms of familial AD are caused by autosomal dominant mutations that often lead to overproduction of Aβ42 peptide. However, the mechanism by which *APOE* alleles differentially modulate Aβ accumulation in sporadic, late-onset AD is less clear. In a cohort of cognitively normal

[*]Please address all correspondence to: Washington University School of Medicine Department of Neurology 660 S. Euclid Ave., Campus Box 8111 St. Louis, MO 63110 holtzman@neuro.wustl.edu Phone: 1-314-362-9872 .
[10]These authors contributed equally to this work.

Author Contributions: J.M.C. wrote and edited the manuscript with critical evaluation/interpretation from co-authors. J.M.C., F.R.S, H.J., D.M.H. performed/designed research in Figs. 1 to 6 and Supplementary Material. A.M.F. and J.C.M. provided human subject data for Fig. 1 and Table 1. C.C., A.M.G., K.R.B. provided human data for Fig S4A. J.K., J.M.C., K.G.M., R.J.B. designed/performed experiments for Fig. 6. J.M.C., J.K., D.M.H. analyzed the data. R.B.D. and S.M.P. contributed valuable reagents.

Competing Interests: D.M.H. and R.J.B. are scientific advisors to C2N Diagnostics, which utilizes the SILK methodology in human studies and are co-inventors on US patent 7,892,845 titled "Methods for measuring the metabolism of neurally derived biomolecules in vivo." Washington University, with D.M.H. and R.J.B. as co-inventors, has also submitted the U.S. non-provisional patent application "Methods for measuring the metabolism of CNS derived biomolecules in vivo," serial #12/267,974. D.M.H. is also on the scientific advisory boards of Satori, En Vivo. D.M.H., J.C.M. and A.M.G. consult for Pfizer and Bristol Myers Squibb. D.M.H. also consults for Innogenetics. J.C.M. also consults for AstraZeneca, Eisai, Janssen, Genentech, Eli Lilly, Merck, Novartis, Otsuka, Schering Plough. A.M.G. also consults for AstraZeneca and Genentech. All other authors declare no competing interests.

individuals, we report that reliable molecular and neuroimaging biomarkers of cerebral Aβ deposition vary in an apoE isoform-dependent manner. We hypothesized that human apoE isoforms differentially affect Aβ clearance or synthesis in vivo, resulting in an apoE isoform-dependent pattern of Aβ accumulation later in life. Performing in vivo microdialysis in a mouse model of β-amyloidosis expressing human apoE isoforms (PDAPP/TRE), we find that the concentration and clearance of soluble Aβ in the brain interstitial fluid depends on the isoform of apoE expressed. This pattern parallels the extent of Aβ deposition observed in aged PDAPP/TRE mice. Importantly, apoE isoform-dependent differences in soluble Aβ metabolism are observed not only in aged PDAPP/TRE mice but also in young PDAPP/TRE mice, well before the onset of Aβ deposition in amyloid plaques. Additionally, amyloidogenic processing of amyloid precursor protein and Aβ synthesis, as assessed by in vivo stable isotopic labeling kinetics, do not vary according to apoE isoform in young PDAPP/TRE mice. Our results suggest that *APOE* alleles contribute to AD risk by differentially regulating clearance of Aβ from the brain, suggesting that Aβ clearance pathways may be useful therapeutic targets for AD prevention.

Introduction

Alzheimer's disease (AD) is the leading cause of dementia in the elderly, with an estimated prevalence of 26 million cases worldwide. Because the number of cases and associated costs are projected to increase dramatically, effective strategies aimed at prevention and preclinical intervention will likely depend on our understanding of how major risk factors contribute to the disease process. The prevailing hypothesis of AD pathogenesis posits that accumulation of brain amyloid-β (Aβ) peptide initiates a pathogenic cascade that culminates in neurodegeneration and dementia (1). The Aβ peptide is generated through sequential proteolytic processing of the amyloid precursor protein (APP) by β- and γ-secretases. Strong biochemical and genetic evidence has demonstrated that most rare, early-onset forms of familial AD are caused by autosomal dominant mutations that result in abnormal processing of APP, leading to overproduction of Aβ or an increase in the ratio of Aβ42 to Aβ40. Much less is known about the factors that initiate or modulate the onset of brain Aβ accumulation in the more common (>99%) sporadic, late-onset form of AD. The best established genetic risk factor for sporadic, late-onset AD is the apolipoprotein E (*APOE*) ε4 allele, the presence of which dramatically increases risk for developing AD and decreases age of onset by 10 to 15 years; in contrast, the *APOE* ε2 allele confers protection against developing AD (2-5). *APOE* status has been found to modulate the onset of extracellular amyloid plaque deposition, one of the key pathognomonic features of the disease (6, 7). Strong evidence demonstrating accelerated onset of amyloid deposition in *APOE* ε4-carriers has led to the hypothesis that *APOE* genotype differentially modulates AD risk and onset through effects on Aβ metabolism (6-9). Consistent with this hypothesis, we and others have reported human apoE isoform-dependent differences in amyloid plaque deposition in APP-transgenic mice (E4 > E3 > E2) (10-14). Although it has been hypothesized that apoE isoforms differentially modulate Aβ accumulation through effects on Aβ clearance, direct in vivo evidence demonstrating apoE isoform-dependent differences in brain Aβ clearance or synthesis has been lacking. Here, we provide in vivo evidence that apoE isoforms differentially modulate brain Aβ burden in a manner that corresponds to early apoE isoform-dependent differences in Aβ clearance. Specifically, we used in vivo microdialysis to measure the concentration of soluble Aβ and its clearance from the brain interstitial fluid (ISF) of young and aged PDAPP/TRE mice. This mouse model of β-amyloidosis overexpresses human APP carrying an autosomal dominant familial AD-linked mutation (V717F) and also expresses each of the human apoE isoforms under the control of the mouse apoE regulatory elements. We found that the soluble Aβ concentration in ISF and its clearance depends on the human apoE isoform expressed in a manner that parallels the pattern of Aβ deposition in old PDAPP/TRE mice. Finally, using an in vivo stable isotopic

labeling kinetics technique, we found no differences in fractional synthesis rates (FSRs) of Aβ among PDAPP/TRE mice, consistent with biochemical evidence suggesting no apoE isoform-dependent changes in amyloidogenic processing of APP. Together, our results provide direct in vivo evidence for a mechanism whereby apoE isoform-dependent differences in Aβ clearance modulate the onset of Aβ accumulation in transgenic mice and in humans.

Results

Biomarkers of cerebral Aβ deposition differ according to *APOE* genotype in humans

Several groups have now validated molecular and neuroimaging biomarkers of the neuropathological hallmarks of AD (15-19). In particular, low concentrations of Aβ42 in the cerebrospinal fluid (CSF) reflect the presence of cerebral Aβ deposition, likely as a result of Aβ42 being sequestered into amyloid plaques, changing the equilibrium between the brain and CSF pools of Aβ (20-22). Additionally, the [^{11}C]-benzothiazole radiotracer, Pittsburgh Compound B (PIB), as well as other tracers, can bind to fibrillar Aβ plaques, allowing for visualization of brain amyloid in individuals during positron emission tomography (PET) (23-25). A preponderance of evidence supports the interpretation that PIB uptake and CSF Aβ42 are reliable surrogate markers of amyloid plaque pathology in living subjects (15-19). A recent study revealed that CSF and neuroimaging biomarkers of amyloid pathology are more prevalent in cognitively normal *APOE* ε4-carriers relative to individuals who have no *APOE* ε4 alleles (that is, have the *APOE* ε3 and/or *APOE* ε2 alleles) (7). Additionally, the *APOE* ε4 allele increases brain amyloid burden assessed by PIB-PET imaging in a gene dose-dependent manner (6). To study the impact of *APOE* ε2, ε3, and ε4 alleles on the development of cerebral Aβ deposition in the absence of AD dementia, we analyzed a cohort of cognitively normal individuals younger than age 70, an age after which the presence of AD dementia may confound the analyses. From this cohort, we analyzed the concentration of Aβ42 in the CSF from *APOE* ε4/ε4, *APOE* ε3/ε4, and *APOE* ε3/ε3 individuals; because *APOE* ε2 homozygous individuals are exceptionally rare, CSF Aβ42 was analyzed in ε2/ε3 individuals. Although various demographic features of our cohort, such as age, sex, and education level, did not differ by *APOE* genotype, the mean concentration of CSF Aβ42 was significantly lower in *APOE* ε4/ε4 individuals compared to individuals of all other *APOE* genotypes in the cohort (Table 1). Given that a CSF Aβ42 concentration lower than 500 pg/mL has been utilized as a reliable threshold for the presence of cerebral Aβ deposition in humans (7, 19, 22, 26), we determined the proportion of individuals in each genotype with CSF Aβ42 lower than 500 pg/mL. We found that there was a significantly greater proportion of *APOE* ε4/ε4 individuals with CSF Aβ42 lower than 500 pg/mL compared to *APOE* ε3/ε4, ε3/ε3, and ε2/ε3 individuals (Fig. 1A). We next identified individuals in the cohort who had received PIB-PET scans within 2 years of lumbar puncture for CSF analysis. On the basis of previous studies (7, 27), individuals with mean cortical binding potential (MCBP) for PIB >0.18 were considered PIB-positive (PIB+). We found that the proportion of PIB+ individuals also follows a strong *APOE* allele-dependent pattern (Fig. 1B). These results demonstrate a clear *APOE* allele-dependent difference in the relative frequency at which individuals exhibit molecular and neuroimaging correlates of amyloid pathology.

Aβ and amyloid deposition in old PDAPP mice is human apoE isoform-dependent

To further investigate the role of apoE isoforms in differentially modulating Aβ metabolism, we used PDAPP mice in which human apoE isoforms are expressed under control of the mouse regulatory elements (PDAPP/TRE) (14). After allowing each cohort of mice to age to 20-21 months, we immunostained brain sections using an anti-Aβ antibody (3D6) and quantified the extent of Aβ deposition covering the hippocampus. Consistent with a previous report (14), we observed marked differences in Aβ deposition depending on the isoform of

apoE expressed (Fig. 2A-C). Quantification revealed that hippocampal Aβ burden in 20- to 21-month-old PDAPP/E4 mice was approximately 2-fold and 4.6-fold higher than in PDAPP/E3 and PDAPP/E2 mice, respectively (Fig. 2D). ApoE is strongly associated with the amount of fibrillar amyloid that deposits into plaques (28). Thus, we next characterized amyloid plaque load in the context of human apoE by staining adjacent brain sections from these mice with X-34, a congophilic dye that binds to amyloid. Consistent with the Aβ immunostaining pattern observed, we found that hippocampal amyloid plaque load varied according to apoE isoform (Fig. 2E-H). Together, these results provide clear evidence that apolipoprotein E4 (apoE4) increases Aβ deposition relative to apoE3 and apoE2 in a manner that closely recapitulates the human biomarker findings reported in Figure 1.

Soluble Aβ concentration and clearance in brain ISF of old mice is human apoE isoform-dependent

To investigate the mechanism by which Aβ accumulation in the brain varies according to apoE isoform in PDAPP/TRE mice, we used in vivo microdialysis to dynamically assess ISF Aβ metabolism in the contralateral hippocampus of PDAPP/TRE mice before harvesting for pathological analysis. The concentration of soluble Aβ in the ISF throughout life has been shown to be closely associated with the amount of Aβ that ultimately deposits in the extracellular space of the brain (29-31). Because soluble ISF Aβ has been shown to closely reflect extracellular pools of Aβ (29-31), we hypothesized that the concentration of soluble Aβ in the ISF would closely follow the pattern of Aβ deposition analyzed from the same mice in Figure 2. Hippocampal ISF was sampled in PDAPP/TRE mice for a stable baseline period during which mice were able to freely behave for the duration of the experiment. We found that the steady state concentration of ISF $Aβ_{1-x}$ (Aβ species containing the N terminus through the central domain of Aβ) varied according to apoE isoform (Fig. 3A). Specifically, the brains of PDAPP/E4 mice had significantly more Aβ in the ISF pool, approximately 2- and 3.8-fold more than PDAPP/E3 and PDAPP/E2 mice, respectively. To understand whether the apoE isoform-dependent differences in soluble Aβ concentration may be the result of altered Aβ clearance from the ISF, we performed clearance microdialysis experiments by analyzing the elimination kinetics of Aβ after halting Aβ production with a potent γ-secretase inhibitor (29) (Fig. 3B). We found that the half-life ($t_{1/2}$) of ISF Aβ in the hippocampus of PDAPP/E4 mice was 1.1 hours, compared to 0.71 and 0.56 hours, measured from PDAPP/E3 and PDAPP/E2 mice, respectively (Fig. 3C). These results demonstrate that the clearance of endogenous Aβ from brain ISF is impaired in old PDAPP/E4 mice relative to PDAPP/E3 and PDAPP/E2 mice.

ApoE isoform-dependent differences in Aβ concentration and clearance exist before Aβ deposition

Because changes in apoE and Aβ metabolism in the brain ISF early in life can markedly alter Aβ deposition later in life (31, 32), we next asked whether the Aβ deposition pattern observed in old PDAPP/TRE mice may be a result of early apoE isoform-dependent differences in ISF Aβ metabolism. To test this hypothesis, we performed in vivo microdialysis in young PDAPP/TRE mice using a sensitive zero flow extrapolation method. Theoretically, the maximum in vivo steady state concentration of an analyte being dialyzed exists at the point at which there is no flow of the perfusion buffer (31, 33). To obtain this value in the hippocampal ISF of PDAPP/TRE mice, we used several flow rates during microdialysis to extrapolate to the point of zero flow for each mouse (Fig. 4A). As shown in Figure 4B, the mean in vivo steady state concentration of soluble ISF Aβ was highest in PDAPP/E4 mice compared to PDAPP/E3 and PDAPP/E2 mice. The concentration of soluble ISF Aβ at each flow rate also varied strongly according to apoE isoform (Fig. S1A). To address the possibility that microdialysis probe function may differ in the context of different human apoE isoforms, we determined the percent recovery at each flow rate, which

revealed no significant differences among PDAPP/TRE mice (Fig. S1B). Since the metabolite urea has been utilized as an independent measure of probe function and recovery in both human and animal brain microdialysis studies (34-37), we measured the concentration of urea in the brain ISF of PDAPP/TRE mice. The concentration of urea did not differ among groups, suggesting that probe function was equivalent across experiments in PDAPP/TRE mice (Fig. S1C). Neither the levels of phosphate-buffered saline (PBS)-soluble Aβ40 nor the levels of murine APP in hippocampal lysates from young apoE knock-in mice expressing murine APP differed according to apoE isoform, suggesting that regulation of Aβ concentration by human apoE may depend on the human Aβ sequence, which differs from murine Aβ by three amino acids (Fig S2A-B). We next asked whether the concentration of the more aggregation-prone Aβ42 species varies according to human apoE isoform in young mice in the ISF pool, the site of Aβ deposition in old PDAPP/TRE mice. We found that the concentration of soluble Aβ42 was highest in young PDAPP/E4 mice compared to PDAPP/E3 or PDAPP/E2 mice (Fig. 4C). We also measured levels of PBS-soluble and PBS-insoluble Aβ40 and Aβ42 after sequential extraction of hippocampi from young PDAPP/TRE mice (Table S1). Although the overall pattern was similar to what we observed in the ISF, the effects were of lesser magnitude or nonsignificant trends were evident, perhaps suggesting the extracted pools we measured do not completely reflect the ISF pool of Aβ (31, 38).

To test the hypothesis that human apoE isoforms differentially regulate the concentration of soluble Aβ in the ISF of young PDAPP/TRE mice through effects on Aβ clearance, we performed clearance microdialysis experiments in young PDAPP/TRE mice. As shown in Figure 4D, Aβ $t_{1/2}$ measured in the hippocampal ISF of PDAPP/E4 mice is significantly longer compared to PDAPP/E3 and PDAPP/E2 mice, respectively. We next assessed Aβ clearance in PS1ΔE9/APPswe/TRE mice, a mouse model of β-amyloidosis based on autosomal dominant AD-linked mutations in *PS1* and *APP* that also expresses one of the human apoE isoforms. We also observed a similar pattern of apoE isoform-dependent Aβ clearance in these mice (Fig. S3), suggesting that the clearance impairment in the context of apoE4 is not an artifact of the PDAPP transgene. Together, these results strongly suggest that the reduced clearance of Aβ from the brain ISF of PDAPP/E4 mice contributes to the increased concentration of Aβ in the ISF, likely resulting in earlier Aβ/amyloid plaque deposition. Several studies have indicated that apoE concentration varies by human apoE isoform (39), raising the possibility that altered apoE concentration may be an endophenotype among *APOE* genotypes that regulates *APOE* allele-dependent Aβ metabolism. We analyzed individuals in our cohort whose CSF had been analyzed by multi-analyte profiling, as previously described (40), which revealed that the presence of one ε2 allele of *APOE* was associated with significantly increased concentrations of apoE relative to other *APOE* genotypes (Fig. S4A). The concentration of apoE in the CSF was also significantly lower in *APOE* ε4-carriers (individuals with one or two copies of *APOE* ε4) compared to *APOE* ε3/ε3 individuals, but the concentration of apoE did not differ between those who were *APOE* ε3/ε3 and those who were *APOE* ε4/ε4. Whereas apoE levels from brain homogenates were higher in PDAPP/E2 mice compared to PDAPP/E3 or PDAPP/E4 mice, levels did not differ between PDAPP/E3 and PDAPP/E4 mice (Fig. S4B). Together, these results suggest that whereas higher apoE concentration in the context of apoE2 may underlie more rapid Aβ clearance relative to apoE4, apoE concentration is unlikely to underlie Aβ clearance differences observed in the context of apoE3 versus apoE4. Moreover, because the extent of apoE lipidation may also play a role in modulating Aβ accumulation (41), we assessed the size of lipidated apoE particles from the CSF of young and old PDAPP/TRE mice by native polyacrylamide gel electrophoresis (PAGE)/Western blot analysis. Regardless of apoE isoform or age, apoE particles were between 12.2nm and slightly larger than 17nm in size (Fig. S4C).

Amyloidogenic processing of APP does not vary according to human apoE isoform

In the amyloidogenic pathway of APP processing, β-secretase (BACE1) cleaves APP N-terminally at the Aβ domain, leading to the generation of sAPPβ and C99, the latter of which ultimately gives rise to the Aβ peptide. In the context of different human apoE isoforms, amyloidogenic processing of APP may vary according to apoE isoform, contributing to the differences in the concentration of ISF Aβ observed in Figure 4B. To begin to address this possibility, we compared levels of the amyloidogenic metabolite C99 in hippocampal homogenates from young PDAPP/TRE mice. As shown in a representative western blot probed with 82E1 antibody (anti-$A\beta_{1\text{-}16}$), which recognizes C99, relative levels of C99 did not differ among PDAPP/TRE mice (Fig. 5A). Quantification revealed that C99 levels did not vary significantly according to human apoE isoform (Fig. 5B). Additionally, full-length APP levels did not appear to vary significantly among groups (Fig. S5A-B). To further assess whether amyloidogenic processing differs according to apoE isoform, we measured β-secretase activity in hippocampal homogenates from young PDAPP/TRE mice. β-secretase activity was measured by monitoring the fluorescence increase that results from cleavage of a peptide based on the β-cleavage site of APP. On the basis of the quantification shown in Figure 5C, there were no significant differences in reaction velocity among PDAPP/TRE mice, suggesting that apoE isoform-dependent differences in β-secretase activity are unlikely to account for differences in soluble ISF Aβ concentration in young PDAPP/TRE mice. Overall, our results in PDAPP/TRE mice are consistent with a previous in vitro study showing no effect of apoE isoforms on APP processing (42).

Rates of Aβ synthesis do not differ according to human apoE isoform

To sensitively assess the rates of Aβ synthesis in the context of human apoE isoforms in PDAPP/TRE mice, we adapted an in vivo stable isotopic labeling kinetics technique previously described in humans (43). Briefly, young PDAPP/TRE mice were intraperitoneally injected with the stable isotope-labeled amino acid [$^{13}C_6$]-leucine, which crosses the blood-brain barrier and incorporates into newly synthesized APP/Aβ during normal protein synthesis in the central nervous system. We next sacrificed mice at 20 and 40 minutes after the injection and immunoprecipitated total Aβ from brain lysates using HJ5.2, an anti-$A\beta_{13\text{-}28}$ antibody. After trypsin digestion of immunoprecipitated Aβ, samples were submitted to liquid-chromatography mass spectrometry (LC-MS), allowing quantification of the relative abundance of labeled to unlabeled Aβ by analyzing mass shifts of predicted MS/MS ions in the spectra (Fig. 6A). To accurately quantify and calibrate the mass spectrometry signals from mouse brain samples, we used cell-secreted Aβ to generate a standard curve based on a known quantity of Aβ labeled with [$^{13}C_6$]-leucine (Fig. 6B). We next calculated fractional synthesis rates (FSR) of Aβ based on the rate of increase in the amount of labeled to unlabeled Aβ between 20 and 40 minutes after injection, normalized to the average enrichment of plasma leucine. We found no significant differences in Aβ FSRs among young PDAPP/TRE mice (Fig. 6C), strongly suggesting that apoE isoforms do not differentially modulate Aβ synthesis in vivo.

Discussion

Despite significant advances in our understanding of the pathological events leading to AD, the causes of Aβ accumulation are only reasonably well understood for a small subset of individuals with AD who have autosomal dominant mutations, resulting in early-onset, familial AD. Most AD cases are sporadic, and in these individuals, the factors leading to Aβ accumulation are not well understood. Because effective AD treatments will likely depend on intervening during the preclinical (presymptomatic) phase of AD (44, 45), understanding how environmental and genetic risk factors modulate pathological hallmarks of the disease will be critical. The strongest genetic risk factor for late-onset, sporadic AD is the *APOE* ε4

allele, which markedly increases risk and reduces the age of onset (46), likely by accelerating the onset of brain Aβ accumulation (6-9). Indeed, we showed in a cohort of cognitively normal individuals less than 70 years of age that biomarkers of brain amyloid accumulation were present at a relative frequency that corresponded to *APOE* genotype, that is, ε4 > ε3 > ε2. Consistent with this observation, we found that old PDAPP/TRE mice developed Aβ/amyloid deposition in an apoE isoform-dependent pattern, that is, E4> E3> E2, a finding that extends previous reports of apoE isoform-dependent Aβ deposition in various mouse models (10, 11, 13, 14). Because the concentration of Aβ in the extracellular space of the brain reflects a balance between its synthesis and clearance rates, we hypothesized that *APOE* genotype differentially modulates Aβ accumulation through effects on Aβ clearance and/or synthesis. To test this hypothesis, we used novel in vivo methodologies to measure endogenous brain Aβ clearance and synthesis in PDAPP mice expressing human apoE isoforms under control of the endogenous mouse *APOE* promoter. Using in vivo microdialysis, we found that the concentration of ISF Aβ in the hippocampus of young and old PDAPP/E4 mice was greater than in PDAPP/E3 or PDAPP/E2 mice, likely as a result of reduced Aβ clearance in PDAPP/E4 mice. ApoE isoform-dependent Aβ clearance was also observed in PDAPP/TRE mice before the onset of Aβ accumulation. To investigate the impact of apoE isoforms on Aβ synthesis, we developed a sensitive method to measure the FSR of brain Aβ in vivo, adapted from the stable isotopic labeling kinetics technique recently utilized by our group in humans (43). Using this technique, we found that the fractional rates of brain Aβ synthesis from young PDAPP/TRE mice did not differ according to the human apoE isoform expressed, consistent with our biochemical results showing that amyloidogenic processing of APP did not vary by human apoE isoform. Our results strongly suggest that *APOE* genotype differentially modulates the onset of Aβ accumulation via differential regulation of Aβ clearance, although the cellular and molecular mechanisms underlying this regulation remain unclear.

Once the link between *APOE* genotype and AD risk had been described, several groups focused on characterizing the putative apoE/Aβ interaction and the extent to which this interaction influenced the aggregation of Aβ in vitro. While our results suggest that apoE isoforms differentially regulate Aβ accumulation via effects on Aβ clearance, we cannot exclude the possibility that apoE isoforms also modulate Aβ accumulation by directly facilitating Aβ fibrillization. For example, lipid-free apoE4 was found to facilitate Aβ fibrillization in vitro to a greater degree compared to apoE3 [(47, 48); see (39) for a review]. Perhaps due to differences in experimental conditions, others have reported that apoE isoforms inhibit the process of Aβ aggregation (39, 49, 50), making it difficult to interpret whether they differentially modulate Aβ accumulation in vivo. Several in vitro studies have demonstrated that lipidated apoE2 and apoE3 bind Aβ with greater affinity compared to apoE4 (39, 51-54). This observation has prompted some to hypothesize that the stronger interaction between Aβ and apoE2 or apoE3 relative to apoE4 may result in greater Aβ clearance, consistent with the clearance pattern we observed in vivo in the current study. Indeed, several studies have demonstrated that Aβ transport from brain into blood is altered when complexed to human apoE (55, 56). A recent study wherein apoE/Aβ complexes were microinjected into wildtype mouse brain revealed that Aβ bound to apoE4 is cleared more slowly than when Aβ is complexed to apoE3 or apoE2 (56). One study found that antagonizing the apoE/Aβ interaction with a small peptide decreased Aβ pathology in the mouse brain, further suggesting that the apoE/Aβ interaction may be relevant to Aβ clearance in vivo (57). Additional studies are needed to characterize the extent of the apoE/Aβ interaction under more physiological conditions and whether differential apoE/Aβ interactions may underlie our current in vivo results. Aside from Aβ egress from brain to blood, in vitro studies have suggested that cellular uptake and degradation of Aβ may also represent clearance mechanisms that are regulated by human apoE (58-60). One recent in vitro study found that human apoE isoforms differed in their ability to facilitate neprilysin-

mediated degradation of Aβ42 within microglia, with apoE4 being the least effective in facilitating Aβ degradation compared to apoE2 or apoE3 (60).

Although there are some conflicting studies (61), several groups have reported that the concentration of apoE in the brains of human apoE knock-in mice varies in an apoE isoform-dependent manner, that is, E2>E3>E4 (14, 62, 63). Together with our present results, the isoform-dependent pattern of apoE concentration in humans and in mice raises the possibility that apoE concentration alone may play a role in the pattern of Aβ clearance and subsequent Aβ accumulation, though apoE concentration differences are unlikely to completely account for Aβ metabolism differences in the setting of apoE3 versus apoE4 (14). The impact of structural differences among apoE isoforms (64), especially differences in relative affinities for various apoE receptors, may also contribute to differences in Aβ clearance. Future studies delineating the precise contribution of both apoE concentration and isoform may directly bear on therapeutic strategies aimed at targeting apoE. Using a mouse model of human apoE-dependent β-amyloidosis, our present results may be directly relevant to human studies. For example, using in vivo stable isotopic labeling kinetics, our group recently reported that CSF Aβ clearance and not synthesis is impaired in a small cohort of late-onset AD patients, though the effect of *APOE* genotype was not assessed (65). Coupled with this recent finding, our present results motivate further investigation as to whether Aβ clearance in humans is modulated by *APOE* genotype. These findings further motivate the development of therapies that increase brain Aβ clearance.

Materials and Methods

CSF Aβ42, apoE, and PIB-PET assessment in humans

Participants were cognitively normal volunteers (between 43 and 70 years of age at time of participation) for a longitudinal memory and aging study at the Washington University Alzheimer's Disease Research Center. Cognitive status was assessed by clinical evaluation based on whether intraindividual decline existed in performance of typical activity (as a result of loss of cognitive function). "Cognitively normal" corresponds to a "0" on the Clinical Dementia Rating (CDR) scale. TaqMan assays (Applied Biosystems, Foster City, US) for both rs429358 (ABI#C_3084793_20) and rs7412 (ABI#C_904973_10) were used for *APOE* genotyping. The allelic discrimination analysis module of ABI Sequence Detection Software was used for allele calling. Positive controls for the six possible *APOE* genotypes were included on the genotyping plate. Individuals with confirmed causative mutations were excluded. CSF Aβ42 was measured using the Innotest Aβ42 ELISA kit (Innogenetics, Ghent, Belgium) according to previous procedures (7). CSF apoE concentration in individuals from our cohort for whom CSF had been analyzed by the company Rules Based Medicine was quantified using multi-analyte profiling (40). PIB-PET assessment, performed within 2 years of lumbar puncture to collect CSF, was performed as reported previously (27). All procedures were approved by Washington University's Human Protection Office and written informed consent was obtained from all participants prior to study entry.

Animals

Homozygous PDAPP (APPV717F) mice lacking apoE on a mixed background comprised of DBA/2J, C57BL/6J, and Swiss Webster were crossed with mice expressing *APOE* ε2, ε3, and ε4 under control of mouse regulatory elements on a C57BL/6J background (gift from P. Sullivan at Duke University) (14). Resulting mice were intercrossed to generate homozygous PDAPP/TRE mice, which were then maintained via a vertical breeding strategy. Male and female PDAPP/TRE mice were used throughout experiments. For experiments involving TRE mice with murine APP, 2.5 month-old, male littermates on a

C57BL/6J background from each *APOE* genotype were purchased from Taconic. All animal procedures were performed according to protocols accepted by the Animal Studies Committee at Washington University School of Medicine.

Tissue preparation and quantification of Aβ/amyloid burden

In vivo microdialysis was performed in the left hemisphere of 20- to 21-month-old mice, after which mice were immediately perfused transcardially, fixing brains in 4% paraformaldehyde overnight. After placing brains in 30% sucrose, the contralateral (noncannulated) hemisphere was sectioned on a freezing-sliding microtome. Serial 50 μm coronal sections were taken from the rostral anterior commissure through the caudal extent of the hippocampus, staining sections with biotinylated 3D6 antibody (anti-$A\beta_{1\text{-}5}$) for Aβ immunostaining quantification and X-34 dye for amyloid load quantification. Slides were scanned in batch mode using the NanoZoomer slide scanner system (Hamamatsu Photonics), capturing images in brightfield mode (Aβ immunostaining) or fluorescent mode (X-34). NDP viewer software was used to export images from slides before quantitative analysis using Image J software [National Institutes of Health (NIH)]. Using three sections per mouse separated each by 300 μm (corresponding to bregma −1.7, −2.0, and −2.3 mm in mouse brain atlas), we determined the percentage of area occupied by immunoreactive Aβ or amyloid (X-34-positive signal) in a blinded fashion, thresholding each slide to minimize false-positive signal, as described (31).

In vivo microdialysis

In vivo microdialysis in 20- to 21-month-old and 3- to 4-month-old PDAPP/TRE mice was performed essentially as described to assess steady state concentrations of various analytes in the hippocampal ISF with a 38kDa cut-off dialysis probe (Bioanalytical Systems, Inc.) (29, 32). ISF exchangeable $A\beta_{1\text{-}X}$ ($eA\beta_{1\text{-}X}$) was collected using a flow rate of 1.0μl/min, whereas ISF $eA\beta_{x\text{-}42}$ and urea were collected using a flow rate of 0.3μl/min. For clearance experiments, a stable baseline of ISF $eA\beta_{1\text{-}X}$ concentration was obtained with a constant flow rate of 1.0ul/min before intraperitoneally injecting each mouse with 10 mg/kg of a selective γ-secretase inhibitor (LY411,575), which was prepared by dissolving in dimethyl sulfoxide (DMSO)/PBS/propylene glycol. The elimination of $eA\beta_{1\text{-}X}$ from the ISF followed first-order kinetics; therefore, for each mouse, $t_{1/2}$ for eAβ was calculated using the slope, k', of the linear regression that included all fractions until the concentration of eAβ stopped decreasing ($t_{1/2} = 0.693/k$, where $k = 2.303k'$). Microdialysis using the zero flow extrapolated method was performed by varying the flow rates from 0.3μl/min to 1.6μl/min, as described (31). Zero flow data for each mouse were fit with an exponential decay regression with GraphPad Prism 5.0 software (33).

Quantitative measurements of ISF eAβ

Quantitative measurements of Aβ collected from in vivo microdialysis fractions were performed using sensitive sandwich ELISAs. For human $A\beta_{1\text{-}x}$ quantification, ELISA plates were coated with m266 antibody (anti-$A\beta_{13\text{-}28}$), and biotinylated 3D6 antibody (anti-$A\beta_{1\text{-}5}$) was used for detection. For $A\beta_{x\text{-}42}$ ELISAs, HJ7.4 (anti-$A\beta_{35\text{-}42}$) antibody was used to capture, followed by biotinylated HJ5.1 antibody to detect (anti-$A\beta_{13\text{-}28}$).

Biochemical analyses of hippocampal homogenates from young PDAPP/TRE mice

After transcardial perfusion with heparinized PBS, brain tissue was microdissected and immediately frozen at −80°C. Hippocampal tissue was manually dounce-homogenized with 75 strokes in radioimmunoprecipitation assay (RIPA) buffer [50 mM tris-HCl (pH 7.4), 150 mM NaCl, 0.25% deoxycholic acid, 1% NP-40, 1 mM EDTA] containing a cocktail of protease inhibitors (Roche). Total protein concentration in hippocampal homogenates was

determined with a BCA protein assay kit (Pierce). Equivalent amounts of protein (50 μg) were loaded on 4-12% bis-tris gels (Invitrogen) for SDS-PAGE before transferring protein to 0.2-μm nitrocellulose membranes. Immediately after transfer, blots were boiled for 10 min before blocking and incubation with 82E1 antibody (anti-$A\beta_{1\text{-}16;}$ IBL) to detect C99. Loading was normalized by stripping blots and re-probing with α-tubulin antibody (Sigma). Normalized band intensities were quantified using Image J software (NIH).

β-secretase activity in hippocampal lysates was assessed using a commercially available kit (#P2985; Invitrogen) that relies on fluorescence resonance energy transfer (FRET) that results from β-secretase cleavage of a fluorescent peptide based on the APP sequence (Rhodamine-EVNLDAEFK-Quencher). Briefly, 5 μg of protein per sample was mixed with sample buffer and β-secretase substrate, monitoring fluorescence signal every minute for 120 minutes with a Synergy2 BioTek (BioTek Instruments, Inc.) plate reader (Ex_{545nm}/Em_{585nm}). Because the kinetics of the reaction for all samples were reliably linear in the 20- to 60-min interval, reaction velocity [relative fluorescence units (RFUs) per minute] was calculated and reported over this interval for all samples. Specificity of β-secretase activity was validated using a commercially available β-secretase inhibitor.

In vivo stable isotopic labeling kinetics

FSRs of Aβ were measured in hippocampal lysates from young PDAPP/TRE mice with a method adapted from the in vivo stable isotopic labeling kinetics technique we have previously described in humans (43) (detailed Materials and Methods available in the Supplementary Material). Briefly, after mice were injected intraperitoneally with [$^{13}C_6$]-leucine (200 mg/kg), brain tissue harvesting and plasma collection was performed 20 and 40 min after injection. Whole hippocampus was lysed with 1% Triton X-100 lysis buffer containing protease inhibitors, and Aβ in the extracts was immunoprecipitated with HJ5.2 antibody (anti-$A\beta_{13\text{-}28}$). After trypsin digestion of immunoprecipitated Aβ, LC-MS was performed to measure the relative abundance of labeled to unlabeled tryptic Aβ peptide, which was calibrated with a standard curve of Aβ secreted from H4 APP695ΔNL neuroglioma cells. FSR curves were then generated based on the amount of labeled to unlabeled Aβ present 20 and 40 min after [$^{13}C_6$]-leucine injection, normalized to the amount of free leucine in the plasma, which was measured by gas chromatography (GC)-MS.

Statistical analysis

Unless indicated otherwise, differences among group means were assessed using a one-way analysis of variance (ANOVA) followed by Tukey's post hoc test for multiple comparisons when the ANOVA was significant. Levels of significance were indicated as follows: *P<0.05, **P<0.01, ***P<0.001. Analyses were performed using GraphPad Prism 5.0 software; human data were analyzed using SAS 9.2 software.

Supplementary Material

Refer to Web version on PubMed Central for supplementary material.

Acknowledgments

We acknowledge investigators and staff of the ADRC's clinical and genetics cores and the Adult Children Study's Biomarker Core for CSF Aβ42. LY411,575 was a gift from P. C. May (Eli Lilly & Co.). **Funding:** This work was supported by NIH grants AG13956 (D.M.H.), NS034467 (D.M.H.), AG034004 (J.M.C.), P30-NS069329 (J.K.), the American Health Assistance Foundation (J.K., D.M.H.), DK56341 (B.W.P., Nutrition Obesity Research Center), NIH grantsAG05681 (J.C.M.), AG03991 (J.C.M.), AG026276 (J.C.M.), P30-NS069329-01 (C.C.), and K23-AG03094601 (R.J.B.); NIH Neuroscience Blueprint Center Core Grant P30-NS057105; and Eli Lilly and Pfizer to Washington University (D.M.H.).

References and Notes

1. Hardy J, Selkoe DJ. The amyloid hypothesis of Alzheimer's disease: progress and problems on the road to therapeutics. Science. 2002; 297:353–356. [PubMed: 12130773]
2. Corder EH, Saunders AM, Strittmatter WJ, Schmechel DE, Gaskell PC, Small GW, Roses AD, Haines JL, Pericak-Vance MA. Gene dose of apolipoprotein E type 4 allele and the risk of Alzheimer's disease in late onset families. Science. 1993; 261:921–923. [PubMed: 8346443]
3. Saunders AM, Strittmatter WJ, Schmechel D, George-Hyslop PH, Pericak-Vance MA, Joo SH, Rosi BL, Gusella JF, Crapper-MacLachlan DR, Alberts MJ, et al. Association of apolipoprotein E allele epsilon 4 with late-onset familial and sporadic Alzheimer's disease. Neurology. 1993; 43:1467–1472. [PubMed: 8350998]
4. Corder EH, Saunders AM, Risch NJ, Strittmatter WJ, Schmechel DE, Gaskell PC Jr. Rimmler JB, Locke PA, Conneally PM, Schmader KE, et al. Protective effect of apolipoprotein E type 2 allele for late onset Alzheimer disease. Nat Genet. 1994; 7:180–184. [PubMed: 7920638]
5. Verghese PB, Castellano JM, Holtzman DM. Apolipoprotein E in Alzheimer's disease and other neurological disorders. Lancet Neurol. 2011; 10:241–252. [PubMed: 21349439]
6. Reiman EM, Chen K, Liu X, Bandy D, Yu M, Lee W, Ayutyanont N, Keppler J, Reeder SA, Langbaum JB, Alexander GE, Klunk WE, Mathis CA, Price JC, Aizenstein HJ, DeKosky ST, Caselli RJ. Fibrillar amyloid-beta burden in cognitively normal people at 3 levels of genetic risk for Alzheimer's disease. Proc Natl Acad Sci U S A. 2009; 106:6820–6825. [PubMed: 19346482]
7. Morris JC, Roe CM, Xiong C, Fagan AM, Goate AM, Holtzman DM, Mintun MA. APOE predicts amyloid-beta but not tau Alzheimer pathology in cognitively normal aging. Ann Neurol. 2010; 67:122–131. [PubMed: 20186853]
8. Schmechel DE, Saunders AM, Strittmatter WJ, Crain BJ, Hulette CM, Joo SH, Pericak-Vance MA, Goldgaber D, Roses AD. Increased amyloid beta-peptide deposition in cerebral cortex as a consequence of apolipoprotein E genotype in late-onset Alzheimer disease. Proc Natl Acad Sci U S A. 1993; 90:9649–9653. [PubMed: 8415756]
9. Tiraboschi P, Hansen LA, Masliah E, Alford M, Thal LJ, Corey-Bloom J. Impact of APOE genotype on neuropathologic and neurochemical markers of Alzheimer disease. Neurology. 2004; 62:1977–1983. [PubMed: 15184600]
10. Holtzman DM, Bales KR, Tenkova T, Fagan AM, Parsadanian M, Sartorius LJ, Mackey B, Olney J, McKeel D, Wozniak D, Paul SM. Apolipoprotein E isoform-dependent amyloid deposition and neuritic degeneration in a mouse model of Alzheimer's disease. Proc Natl Acad Sci U S A. 2000; 97:2892–2897. [PubMed: 10694577]
11. Fagan AM, Watson M, Parsadanian M, Bales KR, Paul SM, Holtzman DM. Human and murine ApoE markedly alters A beta metabolism before and after plaque formation in a mouse model of Alzheimer's disease. Neurobiol Dis. 2002; 9:305–318. [PubMed: 11950276]
12. Dodart JC, Marr RA, Koistinaho M, Gregersen BM, Malkani S, Verma IM, Paul SM. Gene delivery of human apolipoprotein E alters brain Abeta burden in a mouse model of Alzheimer's disease. Proc Natl Acad Sci U S A. 2005; 102:1211–1216. [PubMed: 15657137]
13. Fryer JD, Simmons K, Parsadanian M, Bales KR, Paul SM, Sullivan PM, Holtzman DM. Human apolipoprotein E4 alters the amyloid-beta 40:42 ratio and promotes the formation of cerebral amyloid angiopathy in an amyloid precursor protein transgenic model. J Neurosci. 2005; 25:2803–2810. [PubMed: 15772340]
14. Bales KR, Liu F, Wu S, Lin S, Koger D, DeLong C, Hansen JC, Sullivan PM, Paul SM. Human APOE isoform-dependent effects on brain beta-amyloid levels in PDAPP transgenic mice. J Neurosci. 2009; 29:6771–6779. [PubMed: 19474305]
15. Rowe CC, Ng S, Ackermann U, Gong SJ, Pike K, Savage G, Cowie TF, Dickinson KL, Maruff P, Darby D, Smith C, Woodward M, Merory J, Tochon-Danguy H, O'Keefe G, Klunk WE, Mathis CA, Price JC, Masters CL, Villemagne VL. Imaging beta-amyloid burden in aging and dementia. Neurology. 2007; 68:1718–1725. [PubMed: 17502554]
16. Jack CR Jr. Lowe VJ, Senjem ML, Weigand SD, Kemp BJ, Shiung MM, Knopman DS, Boeve BF, Klunk WE, Mathis CA, Petersen RC. 11C PiB and structural MRI provide complementary information in imaging of Alzheimer's disease and amnestic mild cognitive impairment. Brain. 2008; 131:665–680. [PubMed: 18263627]

17. Shaw LM, Vanderstichele H, Knapik-Czajka M, Clark CM, Aisen PS, Petersen RC, Blennow K, Soares H, Simon A, Lewczuk P, Dean R, Siemers E, Potter W, Lee VM, Trojanowski JQ. Cerebrospinal fluid biomarker signature in Alzheimer's disease neuroimaging initiative subjects. Ann Neurol. 2009; 65:403–413. [PubMed: 19296504]

18. Fagan AM, Mintun MA, Mach RH, Lee SY, Dence CS, Shah AR, LaRossa GN, Spinner ML, Klunk WE, Mathis CA, DeKosky ST, Morris JC, Holtzman DM. Inverse relation between in vivo amyloid imaging load and cerebrospinal fluid Abeta42 in humans. Ann Neurol. 2006; 59:512–519. [PubMed: 16372280]

19. Fagan AM, Roe CM, Xiong C, Mintun MA, Morris JC, Holtzman DM. Cerebrospinal fluid tau/beta-amyloid(42) ratio as a prediction of cognitive decline in nondemented older adults. Arch Neurol. 2007; 64:343–349. [PubMed: 17210801]

20. Sunderland T, Linker G, Mirza N, Putnam KT, Friedman DL, Kimmel LH, Bergeson J, Manetti GJ, Zimmermann M, Tang B, Bartko JJ, Cohen RM. Decreased beta-amyloid1-42 and increased tau levels in cerebrospinal fluid of patients with Alzheimer disease. JAMA. 2003; 289:2094–2103. [PubMed: 12709467]

21. Clark CM, Xie S, Chittams J, Ewbank D, Peskind E, Galasko D, Morris JC, McKeel DW Jr. Farlow M, Weitlauf SL, Quinn J, Kaye J, Knopman D, Arai H, Doody RS, DeCarli C, Leight S, Lee VM, Trojanowski JQ. Cerebrospinal fluid tau and beta-amyloid: how well do these biomarkers reflect autopsy-confirmed dementia diagnoses? Arch Neurol. 2003; 60:1696–1702. [PubMed: 14676043]

22. Fagan AM, Head D, Shah AR, Marcus D, Mintun M, Morris JC, Holtzman DM. Decreased cerebrospinal fluid Abeta(42) correlates with brain atrophy in cognitively normal elderly. Ann Neurol. 2009; 65:176–183. [PubMed: 19260027]

23. Klunk WE, Engler H, Nordberg A, Wang Y, Blomqvist G, Holt DP, Bergstrom M, Savitcheva I, Huang GF, Estrada S, Ausen B, Debnath ML, Barletta J, Price JC, Sandell J, Lopresti BJ, Wall A, Koivisto P, Antoni G, Mathis CA, Langstrom B. Imaging brain amyloid in Alzheimer's disease with Pittsburgh Compound-B. Ann Neurol. 2004; 55:306–319. [PubMed: 14991808]

24. Ikonomovic MD, Klunk WE, Abrahamson EE, Mathis CA, Price JC, Tsopelas ND, Lopresti BJ, Ziolko S, Bi W, Paljug WR, Debnath ML, Hope CE, Isanski BA, Hamilton RL, DeKosky ST. Post-mortem correlates of in vivo PiB-PET amyloid imaging in a typical case of Alzheimer's disease. Brain. 2008; 131:1630–1645. [PubMed: 18339640]

25. Leinonen V, Alafuzoff I, Aalto S, Suotunen T, Savolainen S, Nagren K, Tapiola T, Pirttila T, Rinne J, Jaaskelainen JE, Soininen H, Rinne JO. Assessment of beta-amyloid in a frontal cortical brain biopsy specimen and by positron emission tomography with carbon 11-labeled Pittsburgh Compound B. Arch Neurol. 2008; 65:1304–1309. [PubMed: 18695050]

26. Tapiola T, Alafuzoff I, Herukka SK, Parkkinen L, Hartikainen P, Soininen H, Pirttila T. Cerebrospinal fluid {beta}-amyloid 42 and tau proteins as biomarkers of Alzheimer-type pathologic changes in the brain. Arch Neurol. 2009; 66:382–389. [PubMed: 19273758]

27. Mintun MA, Larossa GN, Sheline YI, Dence CS, Lee SY, Mach RH, Klunk WE, Mathis CA, DeKosky ST, Morris JC. [11C]PIB in a nondemented population: potential antecedent marker of Alzheimer disease. Neurology. 2006; 67:446–452. [PubMed: 16894106]

28. Bales KR, Verina T, Dodel RC, Du Y, Altstiel L, Bender M, Hyslop P, Johnstone EM, Little SP, Cummins DJ, Piccardo P, Ghetti B, Paul SM. Lack of apolipoprotein E dramatically reduces amyloid beta-peptide deposition. Nat Genet. 1997; 17:263–264. [PubMed: 9354781]

29. Cirrito JR, May PC, O'Dell MA, Taylor JW, Parsadanian M, Cramer JW, Audia JE, Nissen JS, Bales KR, Paul SM, DeMattos RB, Holtzman DM. In vivo assessment of brain interstitial fluid with microdialysis reveals plaque-associated changes in amyloid-beta metabolism and half-life. J Neurosci. 2003; 23:8844–8853. [PubMed: 14523085]

30. Yan P, Bero AW, Cirrito JR, Xiao Q, Hu X, Wang Y, Gonzales E, Holtzman DM, Lee JM. Characterizing the appearance and growth of amyloid plaques in APP/PS1 mice. J Neurosci. 2009; 29:10706–10714. [PubMed: 19710322]

31. Kim J, Castellano JM, Jiang H, Basak JM, Parsadanian M, Pham V, Mason SM, Paul SM, Holtzman DM. Overexpression of low-density lipoprotein receptor in the brain markedly inhibits amyloid deposition and increases extracellular A beta clearance. Neuron. 2009; 64:632–644. [PubMed: 20005821]

32. DeMattos RB, Cirrito JR, Parsadanian M, May PC, O'Dell MA, Taylor JW, Harmony JA, Aronow BJ, Bales KR, Paul SM, Holtzman DM. ApoE and clusterin cooperatively suppress Abeta levels and deposition: evidence that ApoE regulates extracellular Abeta metabolism in vivo. Neuron. 2004; 41:193–202. [PubMed: 14741101]
33. Menacherry S, Hubert W, Justice JB Jr. In vivo calibration of microdialysis probes for exogenous compounds. Anal Chem. 1992; 64:577–583. [PubMed: 1580357]
34. Ronne-Engstrom E, Cesarini KG, Enblad P, Hesselager G, Marklund N, Nilsson P, Salci K, Persson L, Hillered L. Intracerebral microdialysis in neurointensive care: the use of urea as an endogenous reference compound. J Neurosurg. 2001; 94:397–402. [PubMed: 11235942]
35. Hillered L, Vespa PM, Hovda DA. Translational neurochemical research in acute human brain injury: the current status and potential future for cerebral microdialysis. J Neurotrauma. 2005; 22:3–41. [PubMed: 15665601]
36. Brody DL, Magnoni S, Schwetye KE, Spinner ML, Esparza TJ, Stocchetti N, Zipfel GJ, Holtzman DM. Amyloid-beta dynamics correlate with neurological status in the injured human brain. Science. 2008; 321:1221–1224. [PubMed: 18755980]
37. Schwetye KE, Cirrito JR, Esparza TJ, Donald C. L. Mac, Holtzman DM, Brody DL. Traumatic brain injury reduces soluble extracellular amyloid-beta in mice: a methodologically novel combined microdialysis-controlled cortical impact study. Neurobiol Dis. 2010; 40:555–564. [PubMed: 20682338]
38. Kang JE, Lim MM, Bateman RJ, Lee JJ, Smyth LP, Cirrito JR, Fujiki N, Nishino S, Holtzman DM. Amyloid-beta dynamics are regulated by orexin and the sleep-wake cycle. Science. 2009; 326:1005–1007. [PubMed: 19779148]
39. Kim J, Basak JM, Holtzman DM. The role of apolipoprotein E in Alzheimer's disease. Neuron. 2009; 63:287–303. [PubMed: 19679070]
40. Craig-Schapiro R, Kuhn M, Xiong C, Pickering EH, Liu J, Misko TP, Perrin RJ, Bales KR, Soares H, Fagan AM, Holtzman DM. Multiplexed Immunoassay Panel Identifies Novel CSF Biomarkers for Alzheimer's Disease Diagnosis and Prognosis. PLoS One. 2011; 6:e18850. [PubMed: 21526197]
41. Wahrle SE, Jiang H, Parsadanian M, Kim J, Li A, Knoten A, Jain S, Hirsch-Reinshagen V, Wellington CL, Bales KR, Paul SM, Holtzman DM. Overexpression of ABCA1 reduces amyloid deposition in the PDAPP mouse model of Alzheimer disease. J Clin Invest. 2008; 118:671–682. [PubMed: 18202749]
42. Biere AL, Ostaszewski B, Zhao H, Gillespie S, Younkin SG, Selkoe DJ. Co-expression of beta-amyloid precursor protein (betaAPP) and apolipoprotein E in cell culture: analysis of betaAPP processing. Neurobiol Dis. 1995; 2:177–187. [PubMed: 9174001]
43. Bateman RJ, Munsell LY, Morris JC, Swarm R, Yarasheski KE, Holtzman DM. Human amyloid-beta synthesis and clearance rates as measured in cerebrospinal fluid in vivo. Nat Med. 2006; 12:856–861. [PubMed: 16799555]
44. Holtzman DM. Alzheimer's disease: Moving towards a vaccine. Nature. 2008; 454:418–420. [PubMed: 18650906]
45. Perrin RJ, Fagan AM, Holtzman DM. Multimodal techniques for diagnosis and prognosis of Alzheimer's disease. Nature. 2009; 461:916–922. [PubMed: 19829371]
46. Roses AD. Apolipoprotein E alleles as risk factors in Alzheimer's disease. Annu Rev Med. 1996; 47:387–400. [PubMed: 8712790]
47. Ma J, Yee A, Brewer HB Jr. Das S, Potter H. Amyloid-associated proteins alpha 1-antichymotrypsin and apolipoprotein E promote assembly of Alzheimer beta-protein into filaments. Nature. 1994; 372:92–94. [PubMed: 7969426]
48. Wisniewski T, Castano EM, Golabek A, Vogel T, Frangione B. Acceleration of Alzheimer's fibril formation by apolipoprotein E in vitro. Am J Pathol. 1994; 145:1030–1035. [PubMed: 7977635]
49. Beffert U, Poirier J. ApoE associated with lipid has a reduced capacity to inhibit beta-amyloid fibril formation. Neuroreport. 1998; 9:3321–3323. [PubMed: 9831470]
50. Wood SJ, Chan W, Wetzel R. Seeding of A beta fibril formation is inhibited by all three isotypes of apolipoprotein E. Biochemistry. 1996; 35:12623–12628. [PubMed: 8823200]

51. LaDu MJ, Falduto MT, Manelli AM, Reardon CA, Getz GS, Frail DE. Isoform-specific binding of apolipoprotein E to beta-amyloid. J Biol Chem. 1994; 269:23403–23406. [PubMed: 8089103]
52. Yang DS, Smith JD, Zhou Z, Gandy SE, Martins RN. Characterization of the binding of amyloid-beta peptide to cell culture-derived native apolipoprotein E2, E3, and E4 isoforms and to isoforms from human plasma. J Neurochem. 1997; 68:721–725. [PubMed: 9003062]
53. Aleshkov S, Abraham CR, Zannis VI. Interaction of nascent ApoE2, ApoE3, and ApoE4 isoforms expressed in mammalian cells with amyloid peptide beta (1-40). Relevance to Alzheimer's disease. Biochemistry. 1997; 36:10571–10580. [PubMed: 9265639]
54. Tokuda T, Calero M, Matsubara E, Vidal R, Kumar A, Permanne B, Zlokovic B, Smith JD, Ladu MJ, Rostagno A, Frangione B, Ghiso J. Lipidation of apolipoprotein E influences its isoform-specific interaction with Alzheimer's amyloid beta peptides. Biochem J. 2000; 348(Pt 2):359–365. [PubMed: 10816430]
55. Bell RD, Sagare AP, Friedman AE, Bedi GS, Holtzman DM, Deane R, Zlokovic BV. Transport pathways for clearance of human Alzheimer's amyloid beta-peptide and apolipoproteins E and J in the mouse central nervous system. J Cereb Blood Flow Metab. 2007; 27:909–918. [PubMed: 17077814]
56. Deane R, Sagare A, Hamm K, Parisi M, Lane S, Finn MB, Holtzman DM, Zlokovic BV. apoE isoform-specific disruption of amyloid beta peptide clearance from mouse brain. J Clin Invest. 2008; 118:4002–4013. [PubMed: 19033669]
57. Sadowski MJ, Pankiewicz J, Scholtzova H, Mehta PD, Prelli F, Quartermain D, Wisniewski T. Blocking the apolipoprotein E/amyloid-beta interaction as a potential therapeutic approach for Alzheimer's disease. Proc Natl Acad Sci U S A. 2006; 103:18787–18792. [PubMed: 17116874]
58. Beffert U, Aumont N, Dea D, Lussier-Cacan S, Davignon J, Poirier J. Beta-amyloid peptides increase the binding and internalization of apolipoprotein E to hippocampal neurons. J Neurochem. 1998; 70:1458–1466. [PubMed: 9523562]
59. Yang DS, Small DH, Seydel U, Smith JD, Hallmayer J, Gandy SE, Martins RN. Apolipoprotein E promotes the binding and uptake of beta-amyloid into Chinese hamster ovary cells in an isoform-specific manner. Neuroscience. 1999; 90:1217–1226. [PubMed: 10338292]
60. Jiang Q, Lee CY, Mandrekar S, Wilkinson B, Cramer P, Zelcer N, Mann K, Lamb B, Willson TM, Collins JL, Richardson JC, Smith JD, Comery TA, Riddell D, Holtzman DM, Tontonoz P, Landreth GE. ApoE promotes the proteolytic degradation of Abeta. Neuron. 2008; 58:681–693. [PubMed: 18549781]
61. Korwek KM, Trotter JH, Ladu MJ, Sullivan PM, Weeber EJ. ApoE isoform-dependent changes in hippocampal synaptic function. Mol Neurodegener. 2009; 4:21. [PubMed: 19725929]
62. Fryer JD, Demattos RB, McCormick LM, O'Dell MA, Spinner ML, Bales KR, Paul SM, Sullivan PM, Parsadanian M, Bu G, Holtzman DM. The low density lipoprotein receptor regulates the level of central nervous system human and murine apolipoprotein E but does not modify amyloid plaque pathology in PDAPP mice. J Biol Chem. 2005; 280:25754–25759. [PubMed: 15888448]
63. Riddell DR, Zhou H, Atchison K, Warwick HK, Atkinson PJ, Jefferson J, Xu L, Aschmies S, Kirksey Y, Hu Y, Wagner E, Parratt A, Xu J, Li Z, Zaleska MM, Jacobsen JS, Pangalos MN, Reinhart PH. Impact of apolipoprotein E (ApoE) polymorphism on brain ApoE levels. J Neurosci. 2008; 28:11445–11453. [PubMed: 18987181]
64. Hatters DM, Voss JC, Budamagunta MS, Newhouse YN, Weisgraber KH. Insight on the molecular envelope of lipid-bound apolipoprotein E from electron paramagnetic resonance spectroscopy. J Mol Biol. 2009; 386:261–271. [PubMed: 19124026]
65. Mawuenyega KG, Sigurdson W, Ovod V, Munsell L, Kasten T, Morris JC, Yarasheski KE, Bateman RJ. Decreased Clearance of CNS {beta}-Amyloid in Alzheimer's Disease. Science. 2010

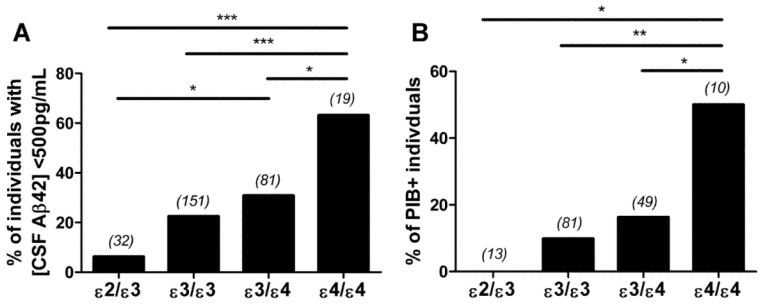

Fig. 1. Biomarkers of amyloid differ according to *APOE* genotype in cognitively normal individuals

(A) Percentage of individuals (n=283) with [CSF Aβ42] < 500 pg/mL according to the following *APOE* genotypes: ε2/ε3, ε3/ε3, ε3/ε4, and ε4/ε4. Number in parentheses indicates number of individuals for each group. **(B)** Percentage of PIB+ individuals (n=153) according to *APOE* genotype: ε2/ε3, ε3/ε3, ε3/ε4, and ε4/ε4. Individuals with mean cortical binding potential for Pittsburgh compound B (MCBP) > 0.18 were considered PIB+. Number in parentheses indicates number of individuals for each group. χ^2 analyses for proportions in (A) ($\chi^2(3)=22.1785$, $P=5.99 \times 10^{-5}$) and (B) ($\chi^2(3)=14.4735$, $P=2.33 \times 10^{-3}$) were performed; follow-up χ^2 tests for pairwise comparisons of proportions were performed using Benjamini and Hochberg's linear step-up adjustment to control for type I error. *P<0.05,**P<0.01,***P<0.001.

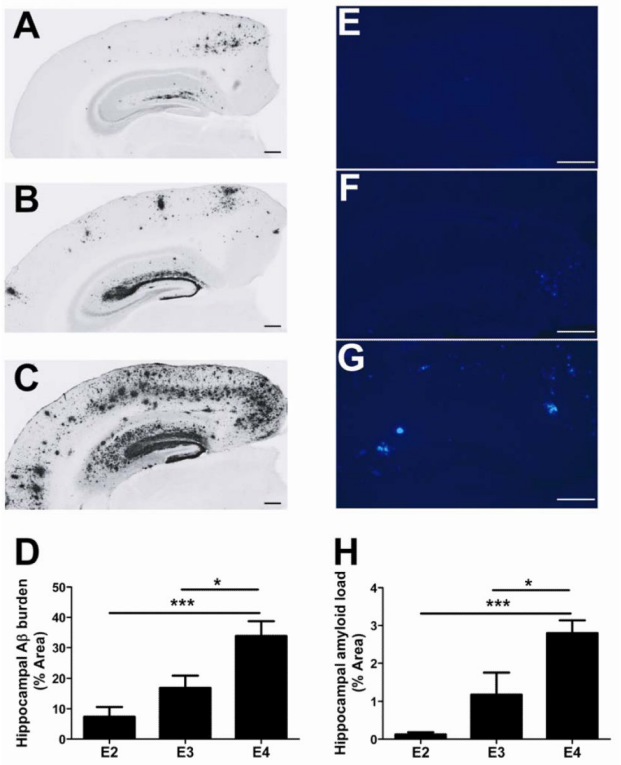

Fig. 2. Aβ/amyloid deposition varies according to apoE isoform in old PDAPP/TRE mice

(A-C) Representative coronal brain sections from 20- to 21-month-old, sex-matched PDAPP/E2 (A), PDAPP/E3 (B), and PDAPP/E4 (C) mice. Aβ immunostaining was performed using anti-Aβ antibody (biotinylated-3D6). Scale bars, 50 μm. **(D)** Quantification of the area of the hippocampus occupied by Aβ immunostaining (n=7 mice/group). *P<0.05, **P<0.01. **(E-G)** Representative coronal brain sections from 20- to 21-month-old PDAPP/E2 (E), PDAPP/E3 (F), and PDAPP/E4 (G) mice. Amyloid was detected using the congophilic fluorescent dye, X-34. Scale bars, 50 μm. **(H)** Quantification of the area of hippocampus occupied by X-34 staining (n=7 mice/group). When one-way ANOVA was significant, differences among groups were assessed using Tukey's post hoc test for multiple comparisons *P<0.05, ***P<0.001. Values represent means ± SEM.

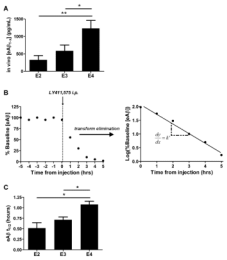

Fig. 3. Soluble Aβ concentration and clearance in the brain ISF of old mice is human apoE isoform-dependent

(A) Mean steady state concentrations of $eA\beta_{1\text{-}X}$ (exchangeable Aβ) from sampling hippocampal ISF in old, sex-matched PDAPP/E2, PDAPP/E3, and PDAPP/E4 mice, measured by enzyme-linked immunosorbent assay (ELISA) (n=6 to 7 mice per group; 20 to 21 months old). **(B)** Schematic diagram of a typical clearance experiment in which a stable baseline period is obtained, followed by intraperitoneal (i.p.) injection of LY411,575 (10mg/kg) to halt Aβ production. Aβ concentrations during the elimination phase are transformed with the common logarithm. Log-transformed values are fit with a linear regression, allowing calculation of slope, k'. $eA\beta\ t_{1/2} = 0.693/k$, where $k = 2.303k'$. **(C)** $eA\beta\ t_{1/2}$ from clearance experiments performed with the mice in (A) after stable baseline measurement of $eA\beta_{1\text{-}x}$. When one-way ANOVA was significant, differences among groups were assessed using Tukey's post hoc test for multiple comparisons (*P<0.05). Values represent means ± SEM.

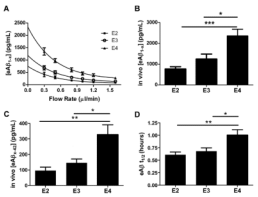

Fig. 4. ApoE isoform-dependent differences in soluble Aβ concentration and clearance exist prior to the onset of Aβ deposition

(A) An exponential decay regression was used to fit the concentrations of $eA\beta_{1\text{-}x}$ measured by ELISA at each flow rate for individual mice from groups of young, sex-matched PDAPP/TRE mice (n=6 mice per group; 3 to 4 months old). The equations from the individual regressions were used to calculate $[eA\beta_{1\text{-}x}]$ at x=0 for each mouse, representing the in vivo concentration of $eA\beta_{1\text{-}x}$ recoverable by microdialysis. **(B)** Mean in vivo concentrations of $eA\beta_{1\text{-}x}$ (pg/mL) calculated from the method in (A). **(C)** Mean concentrations of $A\beta_{x\text{-}42}$ (pg/mL) collected from the hippocampal ISF of young, sex-matched PDAPP/TRE mice using a flow rate of 0.3μl/min (n=8 mice per group; 3-4 months old). **(D)** eAβ $t_{1/2}$ from clearance experiments in young, sex-matched PDAPP/TRE mice after stable baseline measurement of $eA\beta_{1\text{-}x}$ (n=10 to 11 mice per group; 3 to 4 months old). When one-way ANOVA was significant, differences among groups were assessed using Tukey's post hoc test for multiple comparisons *P<0.05, **P<0.01, ***P<0.001. Values represent means ± SEM.

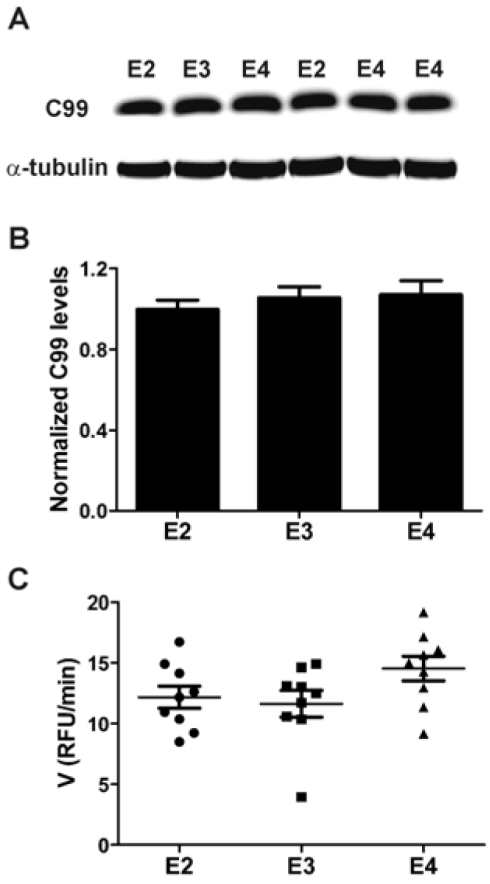

Fig. 5. Amyloidogenic processing of APP does not vary according to human apoE isoform

(A) Representative Western blot of the proximal amyloidogenic metabolite, C99, from hippocampal homogenates (extracted with RIPA buffer) from young, sex-matched PDAPP/TRE mice. C99 was detected using 82E1 antibody. All bands were normalized to α-tubulin band intensity (n=9 mice per group; 3 to 4 months old). **(B)** Quantification of C99 levels after normalizing each band's intensity to α-tubulin band intensity. **(C)** Quantification of β-secretase activity in hippocampal homogenates from young PDAPP/TRE mice using a sensitive FRET assay. Homogenates were incubated with fluorescent APP substrate, resulting in β-cleavage that could be followed by fluorescence increase (emission, 585 nm). The interval over which kinetics were linear was used for quantification of reaction velocity [relative fluorescence units (RFU)/min] for each sample. One-way ANOVA revealed no significant differences among groups. Values represent means ± SEM.

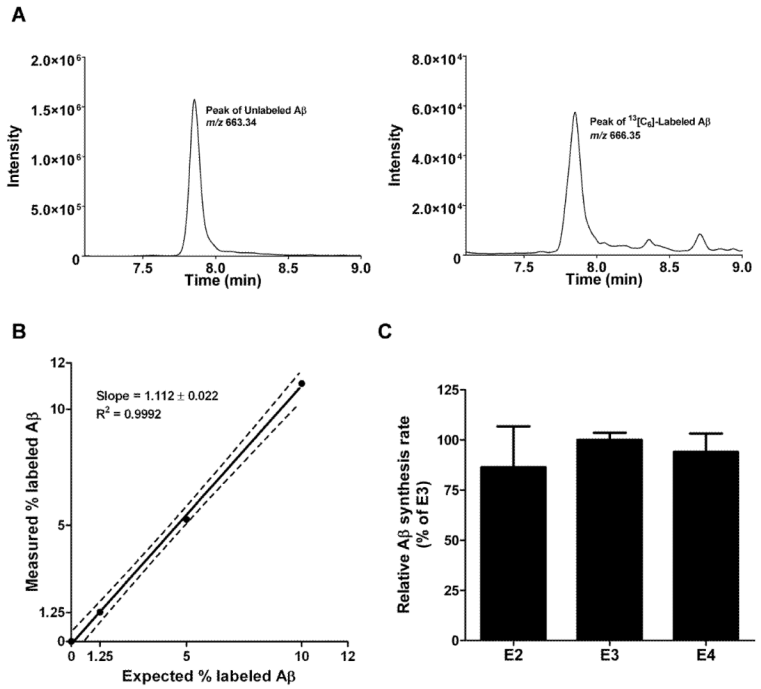

Fig. 6. Rates of Aβ synthesis do not differ according to human apoE isoform in PDAPP/TRE mice

(A) Aβ detection in hippocampal lysates from young PDAPP/TRE mice by TSQ Vantage triple quadrupole mass spectrometry. Left, representative total ion count multiple reaction monitoring (MRM) peak of the unlabeled Aβ tryptic peptide, LVFFAEDVGSNK, (m/z = 663.340). Right, MRM peak for [$^{13}C_6$]-leucine labeled Aβ (m/z = 666.350). **(B)** Standard curve generated with known quantity of [$^{13}C_6$]-leucine labeled and unlabeled Aβ. Aβ secreted from H4-APP695ΔNL neuroglioma cells incubated with labeled/unlabeled leucine was immunoprecipitated with HJ5.2 antibody (anti-$Aβ_{13-28}$), followed by trypsin digestion. $Aβ_{17-28}$ fragments were analyzed on a TSQ Vantage mass spectrometer. The expected percentage of labeled Aβ versus measured percentage was fit by linear regression. Variance is reported with 95% confidence interval. **(C)** Relative FSRs of Aβ from hippocampi of PDAPP/TRE mice intraperitoneally injected with [$^{13}C_6$]-leucine (200mg/kg) (n=5 to 6 mice per group; 4 to 5 months old). Relative FSRs of Aβ were calculated from the ratio of [$^{13}C_6$]-leucine labeled to unlabeled Aβ. [$^{13}C_6$]/[$^{12}C_6$]-Aβ ratio was normalized to the ratio of labeled to unlabeled free leucine in plasma (determined by GC-MS). Mass spectrometry data were normalized with the media standard curve in (B). One-way ANCOVA (analysis of covariance) revealed no significant differences among groups. Values represent means ± SEM.

Table 1

Demographic characteristics and biomarker information for cognitively normal individuals according to *APOE* genotype

Values represent means ± SD. When one-way ANOVA was significant, pair-wise comparisons of *APOE* genotypes were made using Tukey's post hoc test; only significant differences were indicated

	***APOE* genotype**			
	ε2/ε 3	**ε3/ε3**	**ε3/ε4**	**ε4/ε4**
n	32	151	81	19
Female (%)	62.50	64.24	67.90	63.16
Caucasian (%)	87.50	92.05	90.12	84.21
Age at LP, yrs, (SD)	59.28 (7.13)	60.72 (7.17)	60.51 (7.80)	57.58 (8.85)
MMSE	29.28 (0.96)	29.37 (0.94)	29.38 (0.96)	29.32 (1.16)
Education, yrs, (SD)	15.69 (2.76)	15.92 (2.62)	15.83 (2.31)	16.53 (3.42)
Aβ42, pg/mL, (SD)	755.65‡,*** (212.85)	695.58*** (243.87)	619.58** (193.79)	437.39 (183.53)
Tau, pg/mL, (SD)	253.33 (114.68)	248.72 (126.48)	267.54 (131.89)	244.13 (90.58)
pTau, pg/mL, (SD)	50.72 (17.76)	48.18 (19.71)	55.86 (28.83)	51.45 (13.62)

‡ P<0.05,

** P<0.01,

*** P<0.001.

‡ denotes significant difference compared to *APOE* ε3/ε4. ** or *** denotes significant difference compared to *APOE* ε4/ε4. MMSE, Mini Mental State Examination from 0 to 30.